Soft Matter

Dynamic Article Links

Cite this: *Soft Matter*, 2011, **7**, 1690

www.rsc.org/softmatter

COMMUNICATION

Clustering, conductor-insulator transition and phase separation of an ultrasoft model of electrolytes

Daniele Coslovich,*[ab] Jean-Pierre Hansen[c] and Gerhard Kahl[a]

Received 2nd October 2010, Accepted 10th January 2011
DOI: 10.1039/c0sm01090a

We investigate the clustering and phase separation of a model of ultrasoft, oppositely charged macroions by a combination of Monte Carlo and Molecular Dynamics simulations. Static and dynamic diagnostics, including the dielectric permittivity and the electric conductivity of the model, show that ion pairing induces a sharp conductor-insulator transition at low temperatures and densities, which impacts the separation into dilute and concentrated phases below a critical temperature. Preliminary evidence is presented for a possible tricritical nature of the phase diagram of the model.

Clustering of oppositely charged ions is a common mechanism[1,2] which strongly influences the thermodynamic and transport properties of electrolytes, in particular the phase separation into dilute and concentrated ionic solutions predicted to occur at low temperatures.[3] This phase separation (akin to vapour-liquid coexistence) has been investigated in considerable detail both theoretically and by computer simulations in the context of the primitive model of electrolytes, consisting of oppositely charged hard spheres immersed in a dielectric continuum (implicit solvent), with most of the published work focusing on the "restricted" version of the model (RPM) featuring equal anion and cation diameters.[3–7] The RPM is a reasonable model for strong, monovalent electrolytes, like aqueous solutions of NaCl. The formation of long-lived dipolar pairs considerably affects the coexistence curve,[5,8] and severely limits the ergodicity of traditional Monte Carlo (MC) or Molecular Dynamics (MD) simulations at low temperatures.[9]

Recently the attention has shifted to the rich phase behaviour of "colloidal electrolytes" where the anions and cations are highly charged, hard colloidal[10] or nanometric particles,[11] usually in the presence of added salt.[12–14] In this Communication, we extend the RPM to a broader class of soft matter systems by introducing an "ultrasoft" restricted primitive model (URPM), where macroions are assumed to be penetrable charged particles, *i.e.*, the hard cores of charged colloids are replaced by bounded interactions at short interionic distances. Ultrasoft core representations of the effective interaction between the centres of mass (CM) of polymer coils have proved very successful in describing dilute and semi-dilute polymer solutions.[15,16] Our model generalises such a representation to solutions of oppositely charged polyelectrolytes chains.[17,18] We explore, through MC and MD simulations, the subtle interplay between the clustering effects associated with interpenetrating soft core particles[19] and the long-range Coulombic interactions, and its influence on phase separation. Our simulation results for the URPM reveal a non-trivial topology of the phase diagram of the model and suggest a strong link between phase separation and a purely classical conductor–insulator (CI) transition at low temperatures, reminiscent of the behaviour of liquid metals.[20]

The URPM is a system of n_+ cations of total charge $+Q$ and n_- anions of charge $-Q$ per unit volume moving in a dielectric continuum of relative permittivity ε'; global charge neutrality implies $n_+ = n_- = n$. The charge around the CM of each macroion follows a Gaussian distribution $Q_\alpha\rho_\alpha(s) = Q_\alpha\exp[-s^2/2\sigma^2](2\pi\sigma^2)^{-3/2}$ ($\alpha = +$ or $-$) where s is the distance from the CM. The resulting pair potentials as functions of the distance r between the CM's of two ions are:

$$v_{\alpha\beta}(r) = \frac{Q_\alpha Q_\beta}{\varepsilon' r}\mathrm{erf}(r/2\sigma) \underset{r\to 0}{\approx} \pm u_0\left[1 - \frac{r^2}{12\sigma^2} + O(r^4)\right] \quad (1)$$

where $-u_0 = -Q^2/\sqrt{\pi}\varepsilon'\sigma$ is the energy of a fully overlapping anion/cation pair ($r = 0$). For $r \gtrsim \sigma$, the pair potentials go over to the Coulombic interaction between point charges. A related model was used previously to investigated a very different system, namely a semi-classical hydrogen plasma under astrophysical conditions of high temperatures and densities.[21] In the following, we will use $\sqrt{2}\sigma$, u_0, and $\sqrt{2m\sigma^2/u_0}$ as units of length, energy and time, respectively. We will report MC and MD simulations results over a broad range of total density $\rho = 2n$ and temperature T, obtained for samples of $N = N_+ + N_- = 1000$ anions and cations under periodic boundary conditions, employing the Ewald summation technique. Comparison of different simulations methods and different thermal histories provide evidence of proper equilibration of our samples over the investigated range of state parameters.

The classical ground state energy ($T = 0$) is $U = -Nu_0$, which is extensive, ensuring the existence of a proper thermodynamic limit.[22] In the high temperature limit ($T \gtrsim 0.5$) we found that the model is accurately described by the random phase approximation (RPA),

[a]*Institut für Theoretische Physik and CMS, Technische Universität Wien, Vienna, Austria*
[b]*Université Montpellier 2 and CNRS, Laboratoire Charles Coulomb UMR 5221, Montpellier, France. E-mail: daniele.coslovich@univ-montp2.fr*
[c]*Departement of Chemistry, University of Cambridge, Cambridge, United Kingdom*

which reduces to the familiar Debye–Hückel theory for point ions and has been shown to be very accurate also for other soft core models[15,16,19] at high densities.

An interesting phenomenon appears at sufficiently low densities and temperatures, where the system shows clear signatures of clustering. To quantify this phenomenon we first inspect the equilibrium pair structure, which is characterised by the two radial distribution function (RDF) $g_{++}(r) = g_{--}(r)$ and $g_{+-}(r)$. MD data are shown in Fig. 1, along the isochore $\rho = 0.01$, representative of the behaviour of the system at low density. At low T the sharp rise of $g_{+-}(r)$ as $r \to 0$ points to strong anion/cation clustering, as evident in snapshots of ion configurations. Furthermore, clustering at low T is also indirectly evident from $g_{++}(r)$, which appears to imply an attraction between equally charged ions [$g_{++}(r \lesssim \sigma) > 1$]—a fact that can only be rationalised by the formation of tight neutral pairs or higher order clusters.

From the Fourier transforms of the pair correlation functions $h_{\alpha\beta}(r) = g_{\alpha\beta}(r) - 1$ ($\alpha,\beta = +$ or $-$), we extract the charge–charge structure factor

$$S_{CC}(k) = 1 + n\left[\hat{h}_{++}(k) - \hat{h}_{+-}(k)\right] \approx \frac{k^2}{k^2 + \kappa_D^2 \exp\left[-k^2\sigma^2\right]} \text{ (RPA)} \quad (2)$$

where $\kappa_D = (8\pi n Q^2/\varepsilon' k_B T)^{1/2}$ is the inverse Debye screening length, k is the wave-number and hats imply Fourier transforms. The RPA incorporates the exact Stillinger–Lovett sum rule[2] $\lim_{k \to 0} \kappa_D^2 S_{CC}(k)/k^2 = 1$, valid for a conducting medium. The sum rule is well satisfied by our simulation data for $S_{CC}(k)$ along the isochore $\rho = 1$ at all temperatures, and the RPA expression [eqn (2)] provides an accurate representation of the data for all k at sufficiently high T (not shown here). Along the low density isochore $\rho = 0.01$ (see Fig. 2), the RPA expression is accurate only for $T \gtrsim 0.5$ while for $T \lesssim 0.1$, strong deviations from the perfect screening sum rule are observed; fits to the small-k parabolic behaviour of $S_{CC}(k)$ lead to an effective inverse screening length κ systematically larger than κ_D (by a factor of two at $T = 0.025$). This implies that the URPM no longer behaves as a conductor but rather as a dielectric medium of neutral anion/cation clusters.

Using a standard geometric definition of n-ion clusters, namely that n ions form an n-mer if each ion lies within a distance r_c (= 1.0) of at least one other ion in the cluster, we have determined the

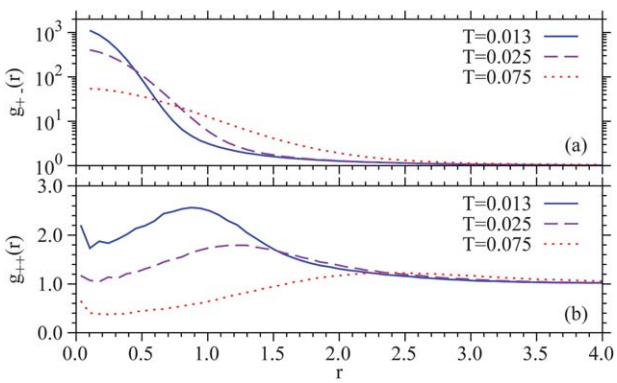

Fig. 1 Radial distribution functions for selected temperatures (as indicated) along the isochore $\rho = 0.01$: (a) $g_{+-}(r)$, (b) $g_{++}(r)$.

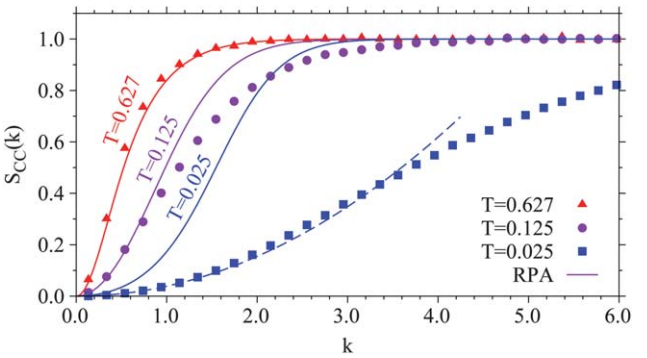

Fig. 2 Charge–charge structure factors $S_{CC}(k)$ for selected temperatures (as indicated) along the isochore $\rho = 0.01$ from MD simulations (filled symbols) and from eqn (2) (solid lines). The dashed line indicates a quadratic fit $(k/\kappa)^2$, where κ is an effective inverse screening length, to the low-k behaviour of $S_{CC}(k)$ for $T = 0.025$.

percentages P_n of n-mers, averaged over all configurations. Examples of P_1 (isolated ions), P_2 (anion/cation pairs) and P_4 (tetramers) as functions of T are shown in Fig. 3-a, along the isochore $\rho = 0.01$. As expected, P_2 is close to 100% at the lowest T, and drops rapidly for $T \gtrsim 0.03$, while P_1 starts from 0 and increases towards 100% for $T \gtrsim 0.03$. Note that the percentage of trimers (now shown) is always negligible while the percentage of tetramers can be significant ($\gtrsim 5\%$ at the lowest temperatures). The lifetime τ_2 of pairs, as estimated from MD simulations, increases dramatically as T drops below 0.05, and is approximately two orders of magnitude larger than that of the other n-mers.

To assess explicitly the effect of pairing on the dielectric properties of the system, we calculate the dielectric permittivity ε from the fluctuations of the total dipole moment of the simulated periodic sample, $\mathbf{M} = \sum_i Q_i \mathbf{r}_i$, according to the standard Kirkwood relation.[23] Results from our simulations along the isochore $\rho = 0.01$ are shown in Fig. 3-b. For $T \lesssim 0.03$ the fluctuations of $\mathbf{M}$ are small, and the

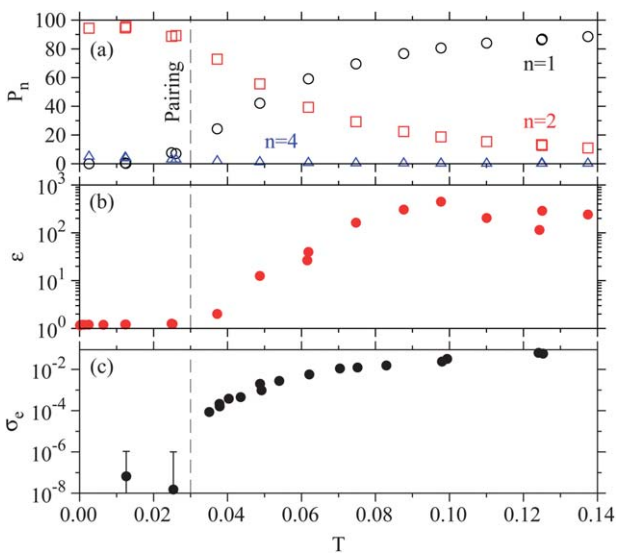

Fig. 3 Comparison of (a) percentages of selected n-mers P_n, (b) dielectric permittivity ε, and (c) conductivity σ_e as functions of T along the isochore $\rho = 0.01$.

resulting ε takes on values of the order of 1.3, typical of dielectrics made up of polarizable molecules (ion pairs in our case). At higher T fluctuations of $\mathbf{M}$ are strongly enhanced, due to the break-up of ion pairs, and ε rises sharply towards values larger than 100, typical of a conductor (for an infinite conducting sample, $\varepsilon \to \infty$).

These suggestions of a CI transition prompted us to extract some dynamic diagnostics from MD simulations.[29] Fig. 4 shows plots of the time-dependent electric dipole diffusion $c(t) = \langle|\mathbf{M}(t) - \mathbf{M}(0)|^2\rangle$. For a conductor, $c(t)$ increases linearly at long times (according to the generalized Einstein relation), and the asymptotic slope is proportional to the electrical conductivity σ_e. At the lowest T, the slope vanishes, *i.e.*, $\sigma_e = 0$, corresponding to a dielectric insulator state. The reduced angular frequency of the oscillations observed at low T is close to the harmonic oscillator frequency of the parabolic anion/cation potential well [eqn (1)], confirming the formation of long-lived pairs that do not contribute to the electrical conductivity. The temperature variation of σ_e is illustrated in the inset of Fig. 4 along two isochores and confirms the sharp drop of σ_e by several orders of magnitude over a narrow range of temperatures. The conductivity data have been fitted by power laws $A(T - T_\sigma)^{1.2}$, yielding the apparent CI transition temperatures $T_\sigma = T_\sigma(\rho)$.

Fig. 3 provides an overview of the behaviour of the system along the representative isochore $\rho = 0.01$, displaying results for the percentages P_n of n-mers, the permittivity ε, and the conductivity σ_e as functions of T. The three plots show a strong correlation between the sharp rise in ε, σ_e and P_1 around $T = 0.03$, indicative of a CI transition, driven by pairing and rounded by finite size effects.

The final step of our investigation is to relate the clustering to the liquid–vapour phase transition expected at low T. To that purpose we have carried out grand-canonical MC simulations in periodic cells of side $L = 9.28$ and $L = 14.7$, combining biased MC sampling and histogram reweighting techniques[24] to construct the coexistence curves shown in Fig. 5, together with the loci of state points where the CI transition is expected (*i.e.*, $\sigma_e \to 0$ according to the aforementioned power law fits) and where the fraction P_1 of free ions reaches 30%. Different choices of the value of P_1 at the pairing transition

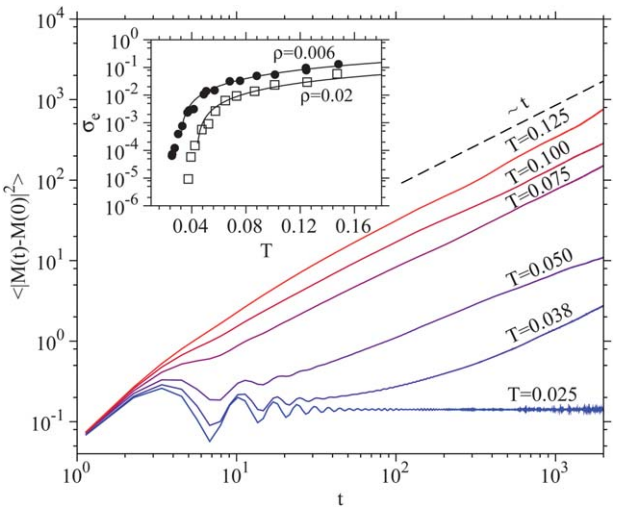

Fig. 4 Diffusion of the total dipole moment $c(t) = \langle|\mathbf{M}(t) - \mathbf{M}(0)|^2\rangle$ as a function of reduced time t for selected temperatures (as indicated) along the isochore $\rho = 0.01$. Inset: electrical conductivity σ_e as a function of T for $\rho = 0.006$ (filled circles) and $\rho = 0.02$ (empty squares). Solid lines are power law fits $\sigma_e(T) \approx A(T - T_\sigma)^{1.2}$.

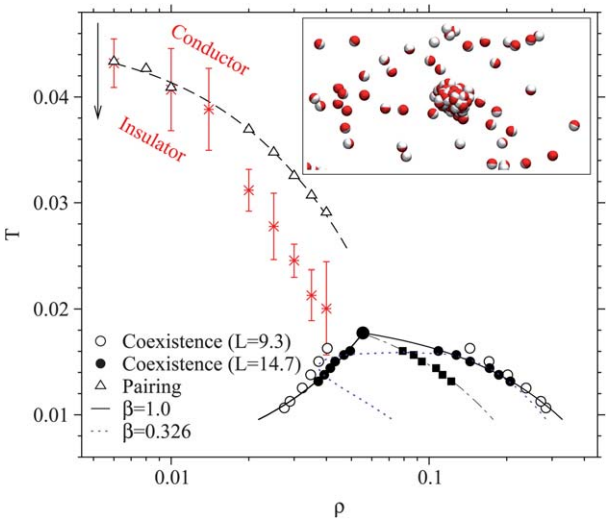

Fig. 5 Extended phase diagram of the URPM: liquid–vapor coexistence from GCMC simulations ($L = 14.7$, filled circles; $L = 9.3$, empty circles), pairing transition points (T_p,ρ_p) determined from the condition $P_1(T_p,\rho_p) = 30\%$ (empty triangles) and CI transition points (T_σ,ρ_σ) (stars; see text for definition). Critical fits to the coexistence curve for $L = 14.7$ are shown for $\beta = 0.326$ (dotted line) or $\beta = 1.0$ (solid line). The estimated critical point corresponding to $\beta = 1.0$ is shown as a bigger filled circle. The law of rectilinear diameter is also included (dash-dotted line and filled squares). The dashed line through the pairing transition points is drawn as a guide to the eye. Inset: MD-generated configuration at $\rho = 0.01$ and $T = 0.00125$. White and red spheres (not drawn to scale) indicate oppositely charged particles.

temperature, as well as variations of r_c by some 10% or 20%, give rise to pairing transition temperatures shifted by at most ± 0.01 with respect to those displayed in Fig. 5. The extrapolation of the two transition lines intersect the coexistence curve close to the critical point, roughly estimated to be $T_c \sim 0.018$, $\rho_c \sim 0.05$ on the basis of the results for $L = 14.7$. The phase diagram shows that the liquid–vapour coexistence curve is better fitted by a scaling law with a critical exponent $\beta = 1$ than by the Ising universality class exponent $\beta = 0.326$ (or by the mean-field exponent $\beta = 0.5$, not shown). Inclusion of corrections to scaling did not improve the fit for $\beta = 0.326$ substantially. The break-down of an Ising-like description of the coexistence curve, the apparent value of the fitted critical exponent ($\beta \approx 1$) and the proximity of the critical point to the CI line hints at a tricritical nature of the phase diagram of the URPM, very different from the Ising-like phase diagram of the RPM. This conjecture will be tested by finite size scaling calculations in future work. We note that the putative tricritical behavior of our model may be different in nature from the one observed in a lattice version of the RPM (see ref. 25 and references therein). The latter behavior is linked in fact to an order–disorder transition, reminiscent of that observed in some antiferromagnetic materials.

As in the case of the RPM, the dilute phase is dominated by long-lived ion pairs (and larger neutral clusters), while in the dense phase, ions are essentially free. This is illustrated by the snapshot in the inset of Fig. 5, which shows droplet formation during an MD simulation at low density and temperature. Identifying the length scales σ of the RPM and the URPM, the reduced critical parameters T_c and ρ_c of the two models are of the same order of magnitude, suggesting that the phase separation is essentially of Coulombic origin. However,

a closer comparison between Fig. 5 and recent simulation results for the RPM[26] reveals a striking difference in the topology of the phase diagram: while in our model the pairing transition line intersects the coexistence curve close to the estimated critical point, pair formation in the RPM represents a crossover occurring at densities much lower than the critical one. Thus the discrepancies between the hard core and soft core models may be traced back to the fundamental difference between long-lived ion pairs at low temperatures and densities: these pairs are strongly dipolar dumbbells in the RPM, while in the present URPM they are non-polar, polarizable entities.

In summary, we have introduced a simple model of oppositely charged, interpenetrating macroions, which generalizes the familiar RPM to "soft" polyelectrolytes. Using static and dynamic diagnostics in MC and MD simulations, we have provided a quantitative characterization of pairing and clustering of ions at low temperatures and densities, and their impact on the segregation into coexisting dilute and concentrated phases. The predicted clustering and segregation of the URPM are reminiscent of the experimentally observed complexation of anionic and cationic polyelectrolytes and subsequent complex coacervation,[17,18] as confirmed by approximate field-theoretic calculations and simulations.[27,28] Examination of the state-dependence of the dielectric pemittivity and of the electric conductivity suggests that pairing leads to a CI transition resembling that observed in liquid metals, such as Hg or Rb. Future work will concentrate on a quantitative analysis of finite size effects and the extension of the URPM to the unrestricted, asymmetric case.

Acknowledgements

We thank C. Valeriani, K. Binder, and S. Clarke for useful discussions. D.C. and G.K. acknowledge financial support by the Austrian Science Foundation (FWF) under Proj. No. P19890-N16.

References

1 N. Bjerrum, *Kgl. Danske Vidensk. Selsk. Mat.-Fys. Medd.*, 1926, **7**, 1.
2 F. H. Stillinger, *J. Chem. Phys.*, 1968, **48**, 3858.
3 A. Z. Panagiotopoulos, *J. Phys.: Condens. Matter*, 2005, **17**, S3205–S3213.
4 G. Stell, K. C. Wu and B. Larsen, *Phys. Rev. Lett.*, 1976, **37**, 1369.
5 Y. Levin and M. E. Fisher, *Physica A*, 1996, **225**, 164.
6 G. Orkoulas and A. Z. Panagiotopoulos, *J. Chem. Phys.*, 1999, **110**, 1581.
7 J.-M. Caillol, D. Levesque and J.-J. Weis, *J. Chem. Phys.*, 2002, **116**, 10794.
8 J. M. Romero-Enrique, L. F. Rull and A. Z. Panagiotopoulos, *Phys. Rev. E: Stat. Phys., Plasmas, Fluids, Relat. Interdiscip. Top.*, 2002, **66**, 041204.
9 C. Valeriani, P. J. Camp, J. W. Zwanikken, R. van Roij and M. Dijkstra, *J. Phys.: Condens. Matter*, 2010, **22**, 104122.
10 M. E. Leunissen, C. G. Christova, A.-P. Hynninen, C. P. Royall, A. I. Campbell, A. Imhof, M. Dijkstra, R. van Roij and A. van Blaaderen, *Nature*, 2005, **437**, 235.
11 J. Ryden, M. Ullner and P. Linse, *J. Chem. Phys.*, 2005, **123**, 034909.
12 A.-P. Hynninen, M. E. Leunissen, A. van Blaaderen and M. Dijkstra, *Phys. Rev. Lett.*, 2006, **96**, 018303.
13 J. B. Caballero, E. G. Noya and C. Vega, *J. Chem. Phys.*, 2007, **127**, 244910.
14 E. Sanz, M. E. Leunissen, A. Fortini, A. van Blaaderen and M. Dijkstra, *J. Phys. Chem. B*, 2008, **112**, 10861.
15 P. G. Bolhuis, A. A. Louis, J.-P. Hansen and E. J. Meijer, *J. Chem. Phys.*, 2001, **114**, 4296.
16 C. Pierleoni, C. Addison, J.-P. Hansen and V. Krakoviack, *Phys. Rev. Lett.*, 2006, **96**, 128302.
17 B. Philipp, H. Dautzenberg, K. J. Linow, J. Koetz and W. Dawydoff, *Prog. Polym. Sci.*, 1989, **14**, 81.
18 H. M. Buchhammer, M. Mende and M. Oelmann, *Colloids Surf., A*, 2003, **218**, 151.
19 C. N. Likos, B. M. Mladek, D. Gottwald and G. Kahl, *J. Chem. Phys.*, 2007, **126**, 224502.
20 F. Hensel, *Adv. Phys.*, 1995, **44**, 3.
21 J.-P. Hansen and I. R. McDonald, *Phys. Rev. A: At., Mol., Opt. Phys.*, 1981, **23**, 2041.
22 D. Ruelle, *Statistical Mechanics: Rigorous Results*, World Scientific Publishing Company, 1999.
23 J. G. Kirkwood, *J. Chem. Phys.*, 1939, **7**, 911.
24 N. B. Wilding, *Am. J. Phys.*, 2001, **69**, 1147.
25 R. Ren, C. J. O'Keefe and G. Orkoulas, *J. Chem. Phys.*, 2006, **125**, 124504.
26 C. Valeriani, P. J. Camp, J. W. Zwanikken, R. van Roij and M. Dijkstra, *Soft Matter*, 2010, **6**, 2793.
27 M. Castelnovo and J. F. Joanny, *Eur. Phys. J. E: Soft Matter Biol. Phys.*, 2001, **6**, 377.
28 J. Lee, Y. Popov and G. Fredrickson, *Eur. Phys. J. E: Soft Matter Biol. Phys.*, 2008, **128**, 224909.
29 Brownian Dynamics simulations would obviously be more appropriate to account for solvent friction, but the more efficient MD, capable of exploring longer time scales was preferred, because we are interested in qualitative, rather than quantitative aspects of the dynamics.